The International Journal of Advanced Manufacturing Technology (2020) 110:1339–1350
https://doi.org/10.1007/s00170-020-05918-2

ORIGINAL ARTICLE

Research on the CNC incremental forming based on multidirectional real-time adjustment of the sheet posture

Hu Zhu[1] · Jilong Li[1]

Received: 25 November 2019 / Accepted: 10 August 2020 / Published online: 23 August 2020

Abstract
There are some problems in the CNC incremental forming with the sheet metal part containing vertical wall, such as excessive thinning and easy fracture. A new CNC incremental forming method was proposed based on the feature recognition for the multidirectional adjustment of the sheet metal posture. According to the feature recognition, the multi-feature of the sheet metal part was decomposed into a number of the forming feature units according to the size and distribution of the forming angles, so that the forming angles of the surface are less than the forming limit angle. The feature recognition and forming feature unit generation algorithm, sheet posture control method, and sheet posture surface generation algorithm were studied, and the finite element analysis and the forming experiments based on the proposed algorithms were also presented. The research results show that the proposed method can change the sheet metal posture in real time during the CNC incremental forming process and realize the non-rupture forming with the large forming angle parts such as vertical wall parts.

Keywords CNC incremental forming · Multidirectional sheet metal posture · Vertical wall · Forming angle

1 Introduction

The sheet metal CNC incremental forming is a flexible and dieless forming technology developed in recent years [1, 2]. This technology uses a squeezing tool to form the sheet metal parts by pressing the sheet layer by layer according to the forming toolpath, which can be widely used in prototype trial production and multi-variety small batch production, and has broad application prospects in aviation, automobile, and shipbuilding industries [3, 4]. However, at present, the difficulty in incremental forming is the forming of the vertical wall part with large forming angle, and the technology still has problems in the forming of the vertical wall part with large forming angle such as excessive thinning and rupture, which seriously restricts the further development of the technology [5, 6]. To overcome the maximum wall angle constraint observed in incremental forming, researchers have explored a variety of multi-stage or multi-pass, toolpath strategies that can improve formability but often cause undesirable stepped features [7].

✉ Hu Zhu
zhuhu10@163.com

[1] College of Mechanical and Electrical Engineering, Shenyang Aerospace University, Shenyang 110136, Liaoning, China

The existing researches [8, 9] show that the thickness t of the sheet is thinned according to the cosine law $t = t_0 \cos\theta$, in which t_0 is the original sheet thickness and θ is the forming angle. In order to solve the problems mentioned above, it is necessary to reduce the forming angle of the vertical wall surface to be less than the forming limit angle. The forming angle θ is the angle between the sheet and the surface of the sheet metal part (Fig. 1a) [10], and its size varies with the sheet posture and the curvature of the surface. In the CNC incremental reverse forming, if the horizontal sheet metal posture (Fig. 1a) is adjusted to the inclined sheet metal posture (Fig. 1b), then the forming angle of the surface is reduced and less than the forming limit angle, which can solve the problem of the sheet cracking due to the excessive thinning.

Therefore, the forming angle can be controlled by adjusting the sheet metal posture, which provides a new solution to the problem that the surface with large forming angles such as vertical walls cannot be formed. The key point is that the sheet metal must be maintained in a reasonable posture with respect to all the features of the surfaces; that is, the forming angle of the surface of the vertical wall should be smaller than the forming limit angle.

However, the horizontal sheet postures are mostly used in the existing CNC incremental forming (Fig. 2a). In recent years, there have been some studies to change the forming

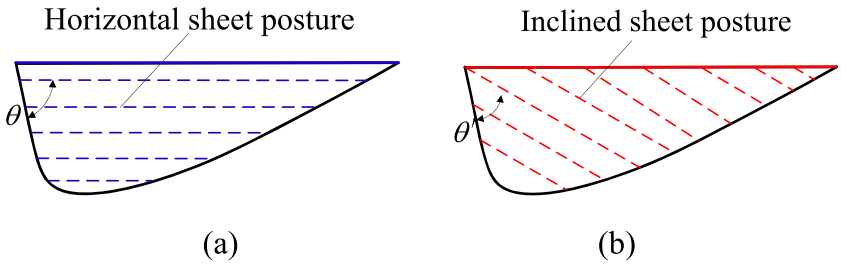

Fig. 1 Relationship of the sheet posture and forming angle: (**a**) before adjustment and (**b**) after adjustment

angle by adjusting the sheet posture. Vanhove et al. [11] and Tanaka et al. [12] studied a method to make the forming angle of the surface to small than the forming limit angle by inclining the sheet metal posture in a certain direction, which was generated by cutting the model using an inclined.

In our previous study [13], for the model of the sheet metal part shown in Fig. 2a (the inclination of the left and right sides is different, and the shape of the front and back sides is symmetrical), the genetic algorithm was used to optimize the inclined sheet metal posture in a certain direction (Fig. 2c), so that each forming angle is smaller than the forming limit angle.

The results show that it is feasible to control the thickness of the formed parts by adjusting the posture of the sheet metal. However, since only a single orientation of the sheet metal posture or the inclined sheet metal posture is used, the method mentioned above can only be applied to the simple shapes such as elliptical cones with different left and right side inclinations as well as the symmetrical front and back shapes and difficult to maintain the sheet to be a reasonable posture with respect to the surfaces having different curvatures. For example, the two vertical wall surfaces of the part shown in Fig. 3 are located in two different features, respectively. Thus, it is not possible to use a single orientation sheet posture to ensure that the forming angles throughout the surfaces are minimized.

In this paper, a new CNC incremental forming method for multidirectional adjustment of the sheet metal posture based on the feature recognition and radial lines is proposed for the multi-feature sheet metal parts with the large forming angles such as vertical wall. The proposed method reduces the forming angle by adjusting the postures of the sheet metal multi-directionally so that the sheet metal part with large forming angle could be formed without the excessive thinning and rupture, which is different from the existing approach that adopts the horizontal sheet posture or adjust the sheet posture only in the single direction.

2 General idea

Since the multi-feature sheet metal parts are generally composed of many forming features with different geometric shapes, it is difficult to minimize the forming angle of the surface by using a certain orientated sheet metal posture. It is necessary to use the combination of the sheet metal postures of each forming feature unit. First, the multi-feature sheet metal parts are decomposed into a plurality of forming feature units as shown in Fig. 4a according to the size and distribution state of the forming angle. Then, each forming feature unit is given a sheet metal posture of different orientations as shown in Fig. 4b, and the sheet metal posture is adjusted in real time by the pressing motion of the squeezing tool so that the forming angle of the surface is smaller than the forming limit angle. Therefore, each of the forming feature units is subjected to different individual forming processes to realize the non-rupture forming of the sheet metal part with a large forming angle such as a vertical wall.

3 Forming feature unit generation based on feature recognition

At present, the researches on the feature recognition mainly focus on the recognition of the cutting features [14–18], but due to the different process requirements, these approaches cannot be applied to the identification of the forming features required for the sheet metal posture adjustment. Lingam et al.

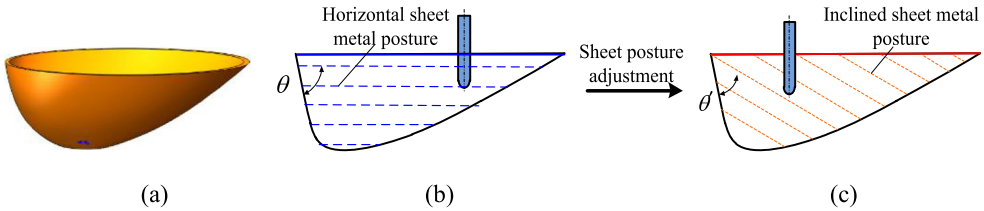

Fig. 2 Previous studies [13]: (**a**) model, (**b**) horizontal sheet metal posture, and (**c**) inclined sheet metal posture

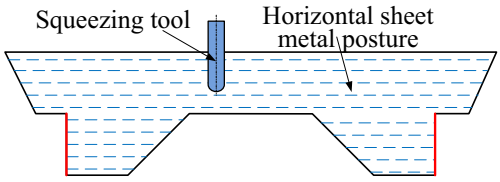

Fig. 3 Single orientation sheet metal posture

[19] studied the identification method based on the support surface feature and the forming surface feature of STEP model in order to switch the function of the main/sub-tool head in double-sided CNC incremental forming, but this method is not suitable for the study. So far, the researches on the identification and generation of the forming features from the perspective of the sheet metal posture adjustment have not been reported in the literature.

In this paper, taking the multi-feature sheet metal parts with the large forming angle surface (such as the vertical wall) as the research object, the forming features were identified and extracted by cutting the triangular mesh model (STL model) that is widely used in the field of the rapid manufacturing area by using the horizontal plane. Under the condition of the CNC incremental reverse forming, any sheet metal part can be classified into the independent feature unit (Fig. 5a, b, c, and d) and nested feature unit (Fig. 5e and f) according to the number and position relationship of the features it contains.

Firstly, for the STL model of the sheet metal part, the upper surface of the sheet metal part is cut from high to low by using the horizontal plane with a certain layer spacing, and the corresponding contour ring is obtained. Then, according to the relationship between the number and relative position of the rings, the forming feature types are distinguished. In the same cutting layer, if there are multiple rings, they can be grouped according to the nesting relationship of each ring. The separation or inclusion relationship between the rings can be judged by checking whether the points in one ring are inside another. If the number of the ring in each layer is 1, it is the independent feature (Fig. 5a, b, and c). Among them, Fig. 5a is the independent feature unit composed of one feature, and Fig. 5b and c is the independent feature units composed of two features. If the number of the rings in a layer is not 1 and the points in one ring of the layer are located inside another ring in the same layer, it is the nested feature (Fig. 5e and f). Among them, Fig. 5e is the nested feature unit composed of two features, and Fig. 5f is the nested feature unit composed of three features (including the independent feature). If the number of the rings in a layer is not 1 and the points of the ring in a layer are not located in the interior of another ring in the same layer, it is the independent feature unit with multiple features. Fig. 5d is the independent feature unit composed of three features. The specific classification algorithm procedure is shown in Fig. 6.

At the same time, the triangular patches connected to the rings arranged from high to low are sequentially extracted, and the normal vector and the forming angle θ_i (i is the number of the triangular patch) of each triangular patch are calculated. The forming features are divided into the difficult-forming surface (its forming angle is larger than θ_{lim}) and the easy-forming surface (its forming angle is smaller than θ_{lim}) according to whether the forming angle is greater than or less than the forming limit angle θ_{lim} [20] (set by the user). Finally, according to the difference of the forming angles of the triangular patches, various features of the part are combined to obtain the forming feature unit. For example, for the independent feature unit shown in Fig. 5b, because the difference of the forming angle from high to low is very big, the features are divided into two types of the features by comparing the forming angles with the θ_{lim}, i.e., the features whose forming angles are larger than θ_{lim} and the other features whose forming angles are smaller than θ_{lim}. The difference of the forming angle of the nested feature unit shown in Fig. 5e is also very big, so it is necessary to compare the forming angle of each surface with the θ_{lim} to distinguish the difficult-forming surface and the easy-forming surface.

4 Sheet metal posture generation for the forming feature unit

4.1 Sheet metal posture generation algorithm

The thickness uniformity of the complex sheet metal part with the difficult-forming surfaces cannot be achieved by a single sheet metal posture, but the multidirectional sheet posture must be adopted. For example, the intermediate raised feature of the flat-top feature (Fig. 7a), the intermediate raised feature under the dashed ring DR of the pointed feature (Fig. 7b), and the left side feature of the independent feature (Fig. 7c) are the difficult-forming surfaces. These surfaces cannot be formed using the horizontal sheet posture but must be formed by the

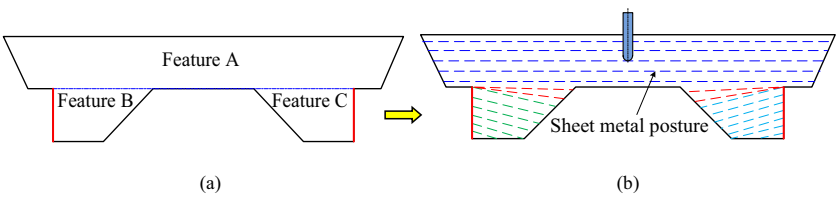

Fig. 4 Proposed method: (**a**) forming features and (**b**) features based multidirectional sheet metal posture

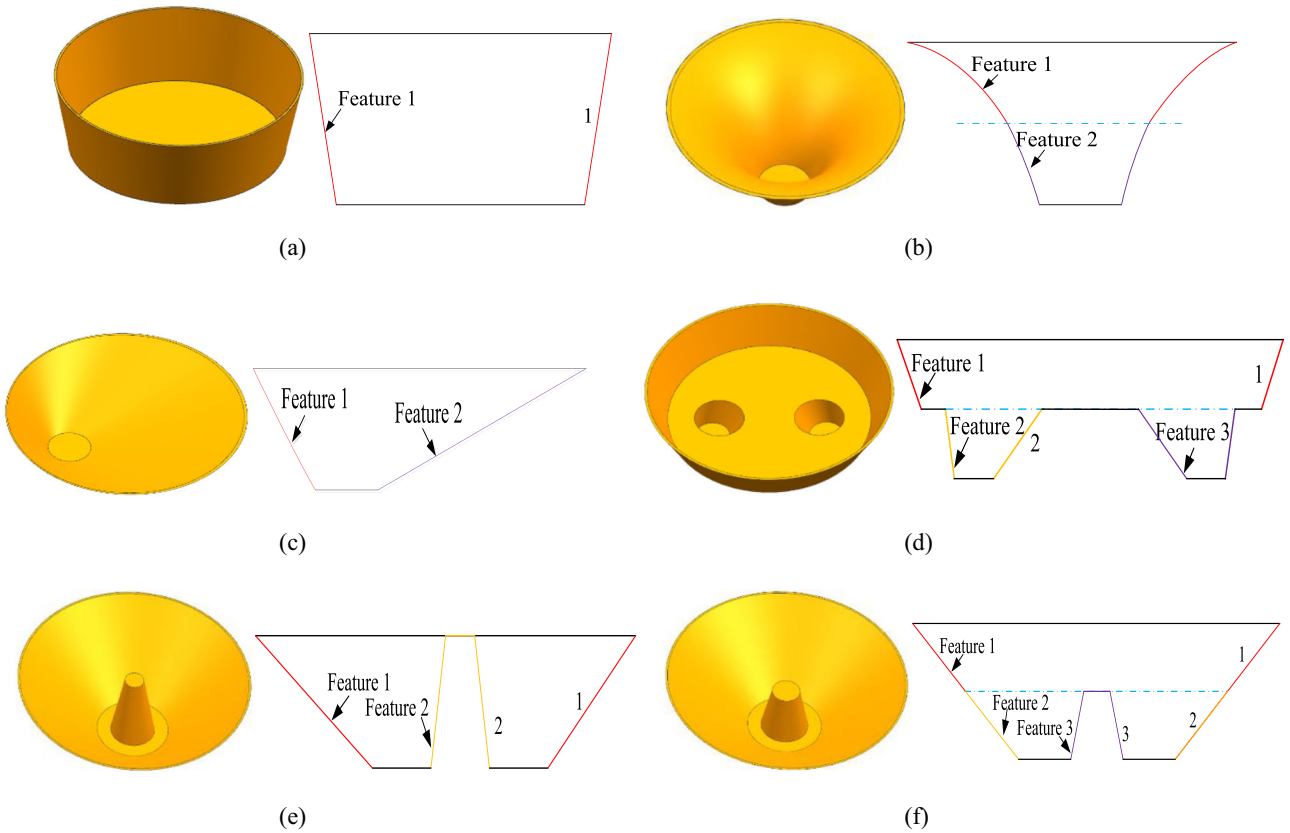

Fig. 5 Sheet metal parts classification: (**a**) independent feature with one feature, (**b**) independent feature with two features, (**c**) independent feature with two features (asymmetric), (**d**) independent feature with three features, (**e**) nested feature with two features, and (**f**) nested feature with three features

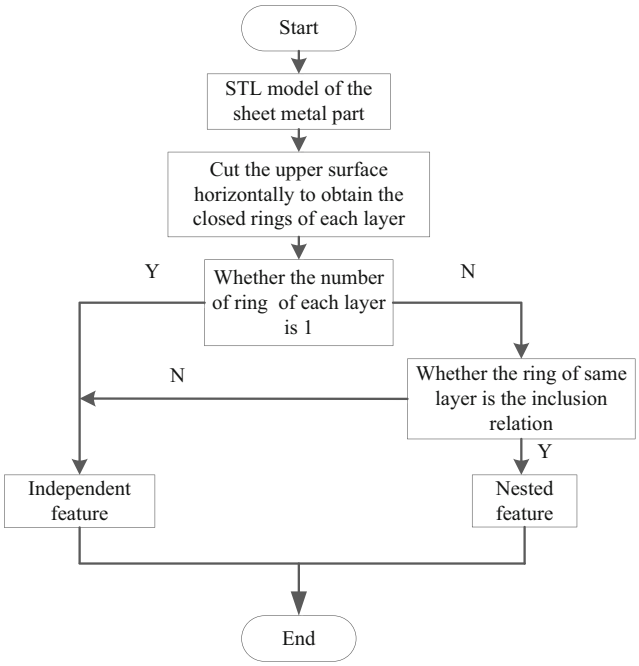

Fig. 6 Sheet metal feature classification algorithm flow

multidirectional adjusted sheet posture so that the forming angles of the difficult-forming surfaces are less than the forming limit angle θ_{lim}.

The detailed algorithm for the generation of the multidirectional adjusted sheet posture is as follows:

1) The contour rings generation. The difficult-forming surface of the model to be formed is cut from high to low using the horizontal plane with a certain spacing h, and a number of tiny line segments are obtained by intersecting the triangular patches with the plane. Then, connect each line segment in turn to obtain a series of contour rings R_i (i = 1, 2, 3 ,..., n, i represents the serial number of the ring). For example, the contour rings of $Surface_1$ from high to low are R_1, R_2, R_3,…R_i…,R_n.
2) Take the points on the contour rings. First, the end points A_{ij} of the line segments of the contour rings are extracted (j = 1, 2, 3, ..., m, j represents the serial number of the points). For example, the end points of the line segments of the contour ring R_i of the $Surface_1$ are sequentially named A_{i1}, A_{i2}, A_{i3} ,… A_{ij}…, A_{im}. Then, it is judged whether the distance between two adjacent points is greater than the

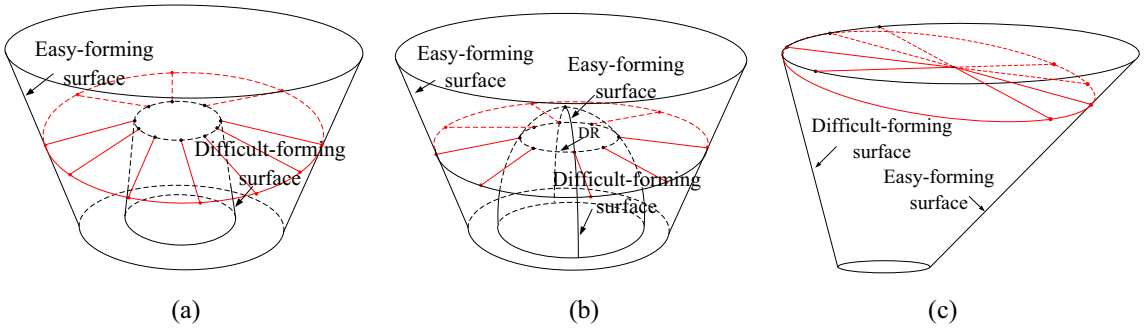

Fig. 7 Sheet posture: (**a**) flat-top feature, (**b**) pointed feature, and (**c**) independent feature

spacing d set by user. If the distance between the two adjacent points is greater than d, the median interpolation method is used to insert a number of points for discretization: First, insert the midpoint of the line segment and determine if the distance between the midpoint and the end of the line segment is greater than d. If it is less than or equal to d, stop the interpolation. If it is greater than d, continue to insert the midpoint of each line segment and determine the distance between the midpoint and the end points of each line segment until it is less than or equal to d.

3) Determination of the center point O_i of each contour ring R_i. The coordinates of the point A_{ij} on the ring are x_{Aij}, y_{Aij}, and z_{Aij}, the area of the ring is S_i (Equation 1), and the coordinates of the point O_i are x_{Oi}, y_{Oi}, and z_{Oi} (Equation 2 and Equation 3), $z_{Oi} = z_{Aij}$.

$$S_i = \frac{1}{2}\sum_{j=1}^{m}\left(x_{ij}y_{ij+1} - x_{ij+1}y_{ij}\right) \tag{1}$$

$$x_{oi} = \frac{1}{6Si}\sum_{j=1}^{m}\left(x_{ij} + x_{ij+1}\right)\left(x_{ij}y_{ij+1} - x_{ij+1}y_{ij}\right) \tag{2}$$

$$y_{oi} = \frac{1}{6Si}\sum_{j=1}^{m}\left(y_{ij} + y_{ij+1}\right)\left(x_{ij}y_{ij+1} - x_{ij+1}y_{ij}\right) \tag{3}$$

4) Generation of the radial lines for each layer. The control center point O_{ij} of the radial line is determined according to the trigonometric function relationship between the center point O_i of the contour ring and the set radial line control angle θ_{ij} (set by user) and the point A_{ij}. A straight line is formed between the control center point O_{ij} and the point A_{ij} on the contour line ring, which intersects with the $Surface_2$ at the point B_{ij}. And the line segment $A_{ij}B_{ij}$ connecting the points A_{ij} and B_{ij} is just the radial line as shown in Figs. 8 and 9.

5) Triangular meshing is performed by using each radial line $A_{ij}B_{ij}$ to generate a multidirectional sheet metal posture surface. For the triangular meshing method, see Section 4.3.

4.2 Transition algorithm between different sheet metal postures

In this study, the CNC incremental forming method based on the multidirectional real-time adjustment of the sheet metal posture is adopted; that is, the different sheet metal postures are adopted for the different feature unit. At this time, the interval between the different sheet metal postures is large, which will affect the forming quality such as the thickness uneven or even cracked. Therefore, it is necessary to study the intermediate sheet metal posture planning method for the smooth transition between the different sheet metal postures (at the boundaries of the different area) of each forming feature unit and generate a sheet metal posture for the transition. For example, as shown in Fig. 10, between the horizontal sheet metal posture D and the inclined sheet metal posture F, a rotated sheet metal posture E is used for the transition.

The generation principle of the transition sheet metal posture is shown in Fig. 11. The detailed generation algorithm is as follows: Firstly, calculate the spacing h_{ij} between the different sheet metal postures (at the junctions of the different area), that is, the difference between the Z coordinate values of the radial line end points A_{1j} and B_{1j} on the first layer of the inclined sheet metal posture surface or the difference between the Z coordinate values of the last radial line endpoints A_{nj} and B_{nj} of the inclined sheet metal posture surface. Secondly, find the maximum spacing h_{ijmax} and determine if it is larger than the spacing h set by the user. If the h_{ijmax} is smaller than the spacing h, then there is no need to add a sheet metal posture surface for the transition; if the h_{ijmax} is larger than the spacing h, insert a number of the sheet metal surfaces for the transition. The method of insertion uses the averaging method to divide

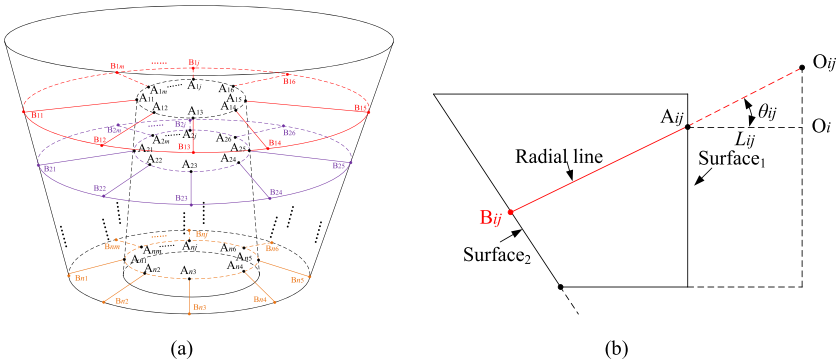

Fig. 8 Radial line generation of the nested features: (a) overall view, (b) partial sectional view

the radial line control angle θ_{ij} at each point of the layer i of the difficult-forming surface corresponding to the h_{ijmax} into h_{max}/h parts (if not an integer, add one to take an integer). Thirdly, determine the control center point O_{ij} of each point A_{ij} according to each control angle and generate each radial line. The method of generating the radial line is the same as the method mentioned in Section 4.1. Finally, the sheet metal posture surfaces for the transition are generated by triangulation of the radial lines. The triangulation method is shown in Section 4.3.

4.3 The sheet metal surface generation algorithm

After a series of the radial lines have been generated in Section 4.1 and Section 4.2, these radial lines need to be triangulated to generate the corresponding sheet metal posture surface. However, since these radial lines are obtained by intersecting the lines that link the control center point of each ring of the difficult-forming surface and each point on the ring with the easy-forming surface, there is a certain angle between two radial lines, which results in the interval between two adjacent points on the easy-forming surface to become larger than the interval between two adjacent points on the difficult-forming surface. If the radial lines are directly triangularly meshed, the chord length will be large, and the generated triangular mesh error will be large. To the end, it may be considered to insert a number of points between two adjacent end points of each radial line on the easy-formed surface and triangulate these points together with the radial line end points. The radial line triangle meshing principle is shown in Fig. 12. The detailed meshing algorithm is as follows: First, the radial line of the layer i is sorted clockwise or counterclockwise and determines whether the distance between two adjacent radial lines $A_{ij}B_{ij}$ and $A_{ij+1}B_{ij+1}$ is larger than the spacing value d_2 (set by the user) between two adjacent points. If the distance between the points B_{ij} and B_{ij+1} is larger than d_2, the median interpolation method is used to insert a number of points for discretization (same as Section 4.1). Second, the adjacent endpoints A_{ij} and B_{ij} of the first line, and the end point A_{ij+1} of the second line on the difficult-forming surface are used as three vertices of the triangular mesh, and the normal vector $\boldsymbol{N}_{ij}$ of the triangular mesh is calculated according to the Equation 4 and Equation 5. Third, the end point B_{ij} on the first line of the easy-forming surface, the end point A_{ij+1} on the second line of the difficult-forming surface, and the first insertion point are used as the three vertices of the triangular mesh, and the normal vector of the triangular mesh is calculated according to above similarly method. By analogy, the calculation is completed when the triangular mesh composed of the last insertion point and the two end points A_{ij+1} and B_{ij+1} of the second line is calculated. Similarly, the triangular mesh composed of the adjacent radial lines is sequentially constructed according to the method mentioned above. Thus, the sheet metal surface of i-layer is generated.

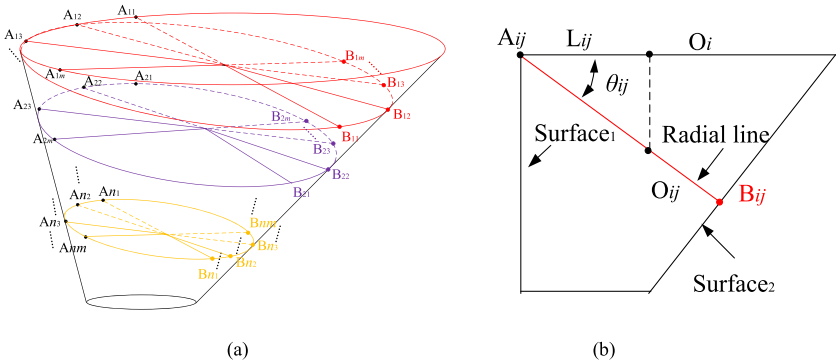

Fig. 9 Radial line generation of the independent features: (**a**) overall view and (**b**) partial sectional view

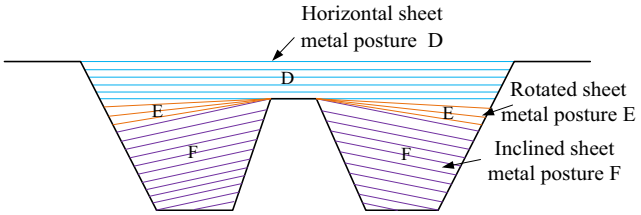

Fig. 10 Transition between the different sheet metal postures

$$Nij = \frac{\overline{AijAij+1}}{\overline{AijBij}} \tag{4}$$

$$Nij+1 = \frac{\overline{BijBij+1}}{\overline{Bij+1Aij+1}} \tag{5}$$

5 Case studies

In order to verify the feasibility of the proposed algorithm, the software system based on the proposed algorithm was implemented by using VC++6.0, C++ language, and OpenGL graphics library on the Windows 7 environment, and the case studies were given by taking the sheet metal part with nested features and independent features, as shown in Fig. 13.

The maximum and minimum forming angle of the sheet metal part are 70.49 and 31.56°, and the difference between the maximum and minimum forming angles is 38.93°. When the forming limit angle is set as 65°, the forming area before feature recombination is as shown in Fig. 14a, and the forming feature units that have been characterized and recombined are as shown in Fig. 14b.

Figure 15a and b shows the contour rings generated by the layer spacing 1 mm and the discrete points obtained by discretizing the contour rings with a 2-mm interval, respectively.

Figure 16 shows the sheet metal surface generated by taking the upper side ring on the difficult-forming surface.

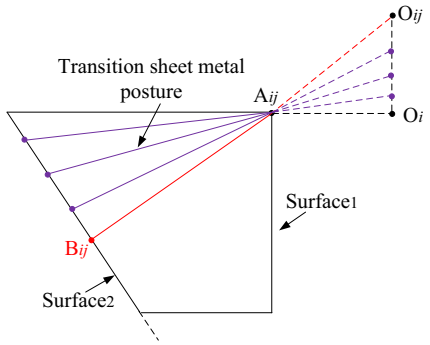

Fig. 11 Sheet metal posture transition

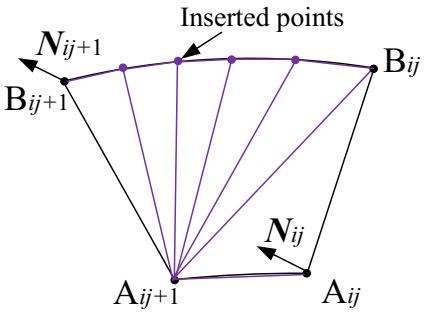

Fig. 12 Triangular meshing based on the radial lines

Figure 16a shows the radial line obtained by intersecting each point on the ring with the easy-forming surface when the radial line control angle is 12°. Figure 16b shows the multidirectional sheet metal surface obtained by triangular meshing using the radial line. The section view of the multidirectional sheet metal surface is shown in Fig. 16c.

Figure 17a shows the radial lines of the sheet metal surface for the transition were generated at the intervals 3° of the control angle. Figure 17b shows the sheet metal surface for the transition obtained by triangular meshing using the radial lines. Figure 17c shows the section view of the model.

5.1 Finite element analysis

In this paper, taking the nested feature model shown in Fig. 13 and the sheet metal posture adjustment angle of 12° as an example, the numerical simulation analysis was carried out by using the finite element analysis software ANSYS/LS-DYNA. In the creation of the finite element analysis unit, the support mold and squeezing tool head used the "SOLID164" three-dimensional display unit, the sheet metal used the "SHELL 163" shell unit, and the shell element algorithm used the "Belytschko-Wong." For the real constant definition of the sheet metal, the shear factor "Shear Factor" was set to 5/6, the integration point number "No. of integration pts" was set to 5, and the sheet thickness "Thickness at node 1" was set to 0.88 mm. The material of the sheet metal was the 1060 aluminum, the squeezing tool head was set to the spherical tool head with a radius of 5 mm, and the tool head was

Fig. 13 The model of the sheet metal part

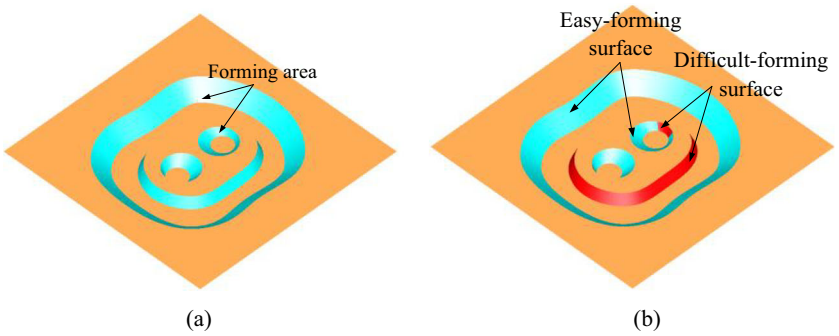

Fig. 14 Forming features: (**a**) before partitioning and (**b**) after partitioning

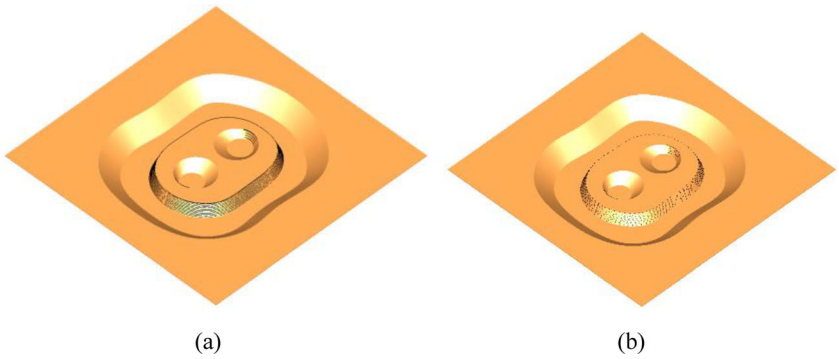

Fig. 15 (**a**) Contour ring and (**b**) contour ring discretization

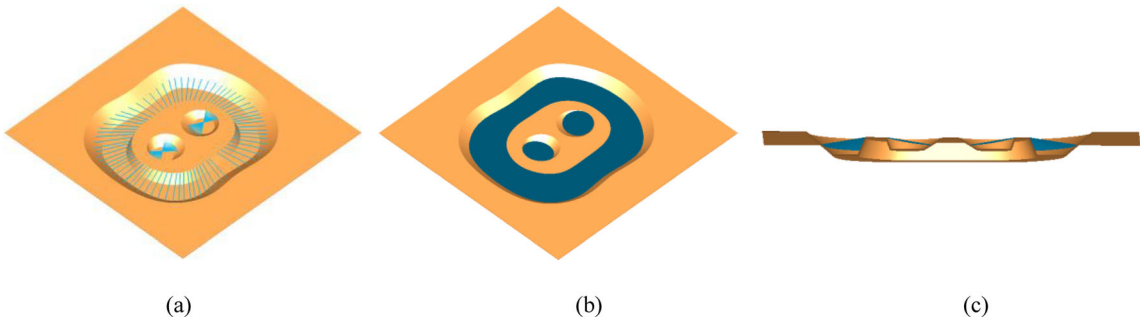

Fig. 16 Multidirectional sheet metal posture: (a) radial line, (b) sheet metal surface, (c) section view

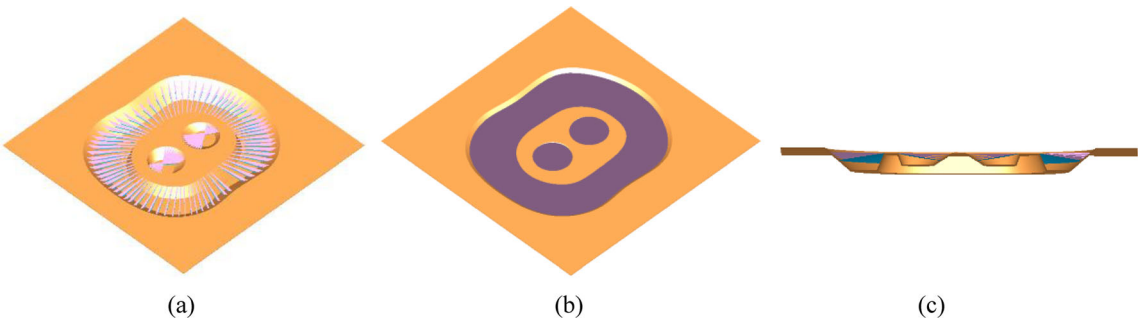

Fig. 17 The sheet metal posture for the transition: (**a**) radial line, (**b**) sheet metal surface, and (**c**) section view

Table 1 Material mechanical properties

Name	Density/ kg•m-3	Elastic modulus/Gpa	Poisson's ratio	Yield stress/Mpa	Tangent modulus/Gpa	Hardening coefficient
Sheet metal	2700	55.94	0.324	153.6	2.9	0.19775
Tool head	8160	218	0.30	----	----	-----
Support mold	7810	212	0.29	----	----	-----

made of the W6Mo5Cr4V2 high speed steel, and the support mold was made of the bearing steel of GCr15. The mechanical properties of each material are shown in Table 1.

The sheet metal, the squeezing tool head, and the support mold were meshed using the 1.5 mm mapped mesh, the 1.5 mm free mesh and the 4 mm free mesh, respectively. The static friction factor of the tool head in contact with the sheet metal was set to 0.1, the dynamic friction factor was set to 0.05; the static friction factor of the sheet metal contact with the support mold was set to 0.5, and the dynamic friction factor was set to zero. At the same time, 6° of freedom of rotation and translation of the sheet metal and the support mold were constrained; 3° of freedom of the rotation of the tool head was constrained. Figure 18 shows the finite element analysis process based on the multidirectional sheet metal posture.

Figure 19 shows the thickness distribution cloud figure obtained by the numerical simulation. It can be seen from the figure that the thickness of the difficult-forming area is between 0.2384 and 0.4329 mm. The thickness of the easy-forming area is between 0.4977 and 0.6922 mm.

In order to analyze the contour precision of the numerical simulation part, the coordinate value of the point on the contour line of the intermediate section of $Y = 0$ was extracted by taking the center point O_1 of the upper ring of the difficult-forming surface as the coordinate origin. The intermediate section profile curve of $Y = 0$ is compared with the intermediate section profile curve of $Y = 0$ of the theoretical model as shown in Fig. 20. To further compare the degree of the difference between the theoretical and the simulated model contour, the Z-direction deviation curve of the two contour lines on the $Y = 0$ section is shown in Fig. 21.

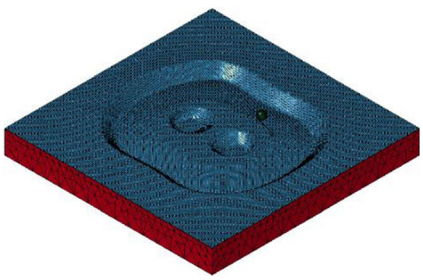

Fig. 18 Finite element analysis based on the multidirectional sheet metal posture

5.2 Forming experiment

In order to further investigate the influence of the sheet metal posture adjustment on the forming quality of the formed part, the nested feature model shown in Fig. 13 was taken as the test part, and the forming experiment was carried out with the sheet metal posture adjustment angle of 12°. In the experiment, the support mold was made of the chemical wood and milled by using the mold engraving machine. The sheet metal was the 1060 aluminum plate with the thickness of 0.88 mm. The squeezing tool head was the hemispherical shape with the diameter of 10 mm. The spindle speed and the feed rate were set as 400 r/min and 600 mm/min, respectively. Figure 22a shows the sheet metal posture at the initial stage of the forming process. Figure 22b and c shows the situation in which the sheet metal posture is continuously adjusted during the forming process and the finally formed part, respectively.

In order to analyze the influence of the posture adjustment of the sheet metal on the contour accuracy of the part, the contour of the part was measured with the CMM. The center point O_1 of the upper ring on the difficult-forming surface was taken as the coordinate origin, and the coordinate value of the point on the contour line of the middle section $Y = 0$ of the forming part was measured at an interval of 2 mm. Then the

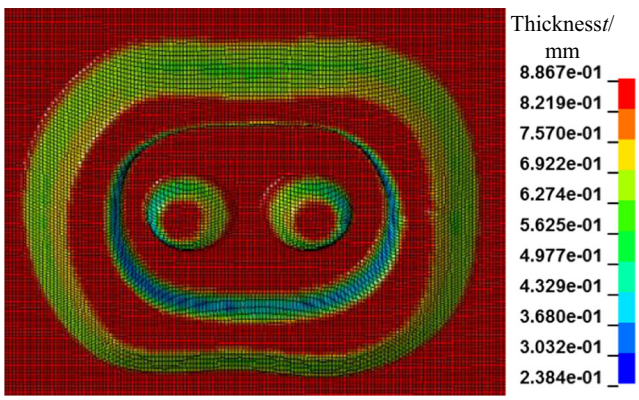

Fig. 19 Thickness distribution cloud

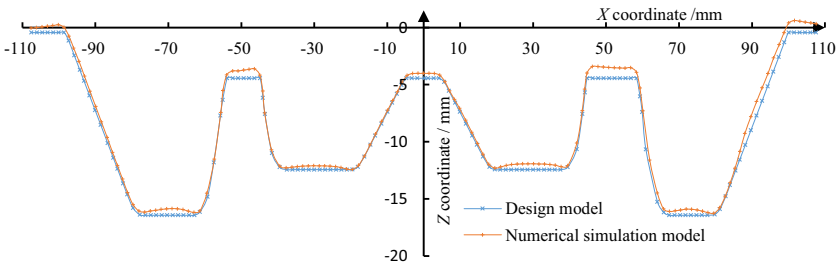

Fig. 20 $Y = 0$ section profile curve

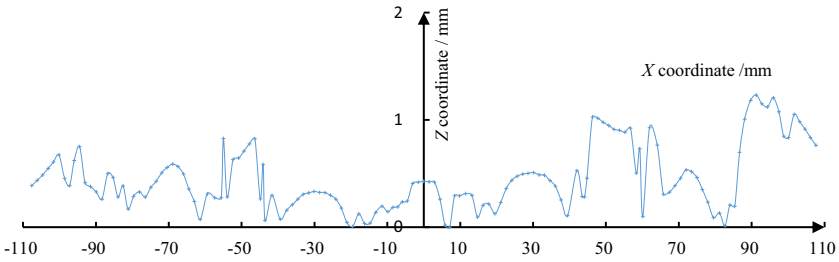

Fig. 21 Z-direction deviation

contour curve was compared with the contour curve of the theoretical model (Fig. 23). In order to further compare the degree of the difference between the contours of the theoretical model and formed part, the Z-direction deviation curve of the section $Y = 0$ was drawn in Excel, as shown in Fig. 24.

It can be seen from Figs. 23 and 24 that the contours of the easy-forming surfaces of the formed part and the theoretical model are in good agreement except for areas A, B, and C (Fig. 25). Because the sheet postures for the transition and the toolpath for pressing the sheet to the bottom were not set in areas A and C, the sheet could not be extruded to the bottom by pressing movement of the forming tool, which lead to undercuts in areas A and C. The undercuts in the area A and C cause a certain dimension deviation in the area B.

In order to analyze the thickness reduction, the formed part was cut into two pieces along the $Y = 0$ section using the wire cutter as shown in Fig. 26a. The mark points were made at 2-mm interval from the bottom to top along the $Y = 0$ section as shown in Fig. 26b, and the thickness at the mark points was measured using the double pointed micrometer as shown in Fig. 26c.

Fig. 22 Forming experiment: (**a**) horizontal posture, (**b**) multidirectional posture, (**c**) formed part

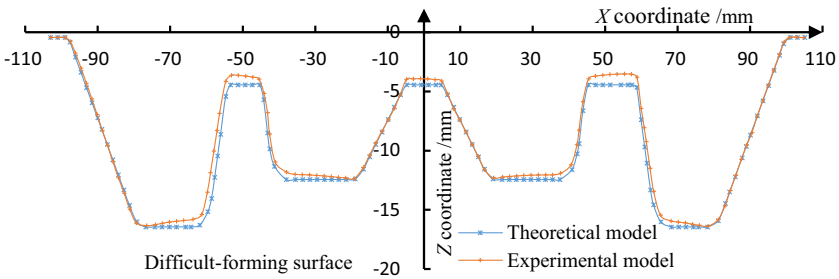

Fig. 23 $Y = 0$ section profile curve

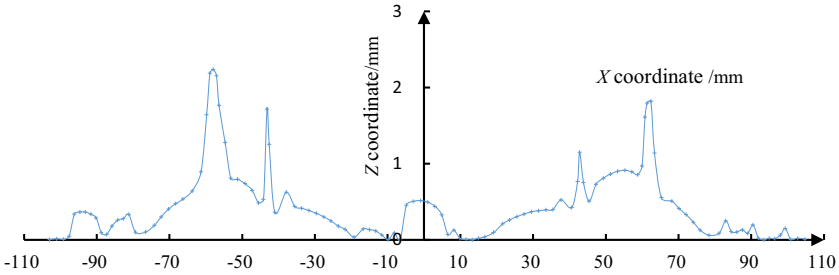

Fig. 24 *Z*-direction deviation

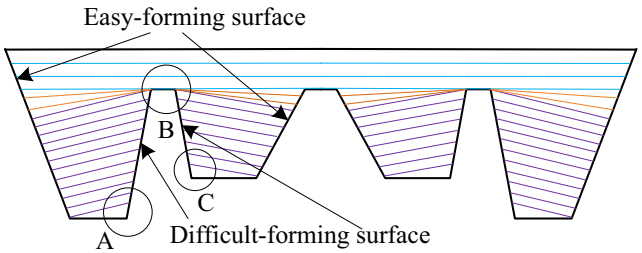

Fig. 25 Tilted sheet posture

The overall thickness thinning of the formed part is not big, but the local thinning is obvious as shown in Fig. 27. The maximum thinning is located at the bottom of the difficult-forming surface of the nested feature and the independent feature, and the minimum thickness and the average thickness are 0.245 mm and 0.771 mm, respectively.

In the forming process, the forming angles of the difficult-forming surface were reduced 12° by tilting the sheet posture from difficult-forming surface to easy-forming surface and were less than the forming limit angle of the material, which made the vertical wall part that cannot be formed by the conventional CNC incremental forming to be formed successfully. The effectiveness of the proposed method can be seen from the results of the FEM simulation and the forming experiment.

6 Conclusion

In this paper, a new CNC incremental forming method with the multidirectional adjustment of the sheet metal posture based on the feature recognition was proposed to solve the constraint in forming of the vertical wall part with large forming angle. The research results show that the proposed method can change the sheet metal posture in real time during the CNC incremental forming process and realize the non-rupture forming of the sheet metal part with large forming angle such as vertical wall. The sheet metal part formed by the multidirectional adjustment of the sheet metal posture has a certain deviation compared with the theoretical model in the contour, but the overall deviation is not large and the surface

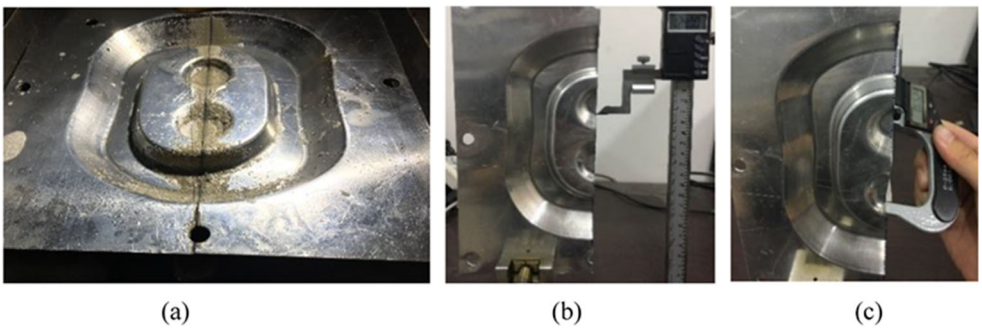

Fig. 26 Formed part: (**a**) cutting process, (**b**) points marking, and (**c**) thickness measurement

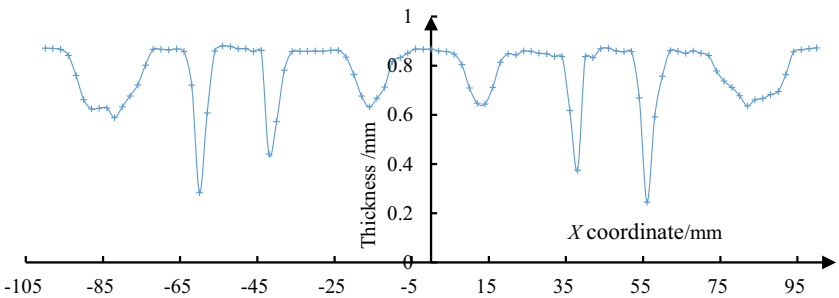

Fig. 27 Thickness distribution curve

forming quality is very good. The overall thickness reduction of the formed part is also not large. The proposed method can effectively overcome the bottleneck problem of the existing CNC incremental forming, such as the thickness of the formed parts is too thin and the vertical walls cannot be formed. In the future research, it is necessary to study the adjustment method of the optimal combination of the multidirectional sheet metal postures, which can minimize and homogenize the thickness of the formed parts. The sheet postures and the toolpath for the bottom of the sheet metal part are also necessary to be studied.

References

1. Behera AK, Sousa RA, Ingarao G (2017) Single point incremental forming: An assessment of the progress and technology trends from 2005 to 2015. J Manuf Process 27:37–62
2. Li YL, Chen XX, Liu ZB, Sun J, Li F, Li JF, Zhao GQ (2017) A review on the recent development of incremental sheet-forming process. Int J Adv Manuf Technol 92(5-8):2439–2462
3. Tisza M (2012) General overview of sheet incremental forming. Mater Des 55(1):113–120
4. Leacock AG (2012) The future of sheet metal forming research. Mater Manuf Process 27(4):366–369
5. Ambrogio G, Filice L, Gaudioso M, Manco GL (2010) Optimized tool-path design to reduce thinning in ISF process. Int J Mater Forming 3(1):959–962
6. Xiaoqiang L, Kai H, Xu P, Wang H, Dongsheng L, Yanle L, Qing L (2020) Experimental and theoretical analysis of the thickness distribution in multistage two point incremental sheet forming. Int J Adv Manuf Technol 107(1-2):191–203
7. Ndip-Agbor E, Cheng P, Moser N, Ehmann K, Cao J (2019) Prediction of rigid body motion in multi-pass single point incremental forming. J Mater Process Technol 269:117–127
8. Young D, Jeswiet J (2004) Wall thickness variations in single point incremental forming. J Eng Manuf 218(11):1453–1459
9. Hirt G, Ames J, Bambach M, Kopp R (2004) Forming strategies and process modelling for CNC incremental sheet forming. Ann CIRP 53(1):203–206
10. Shankar R, Jadhav S, Gobel R (2005) Incremental sheet metal forming of preformed sheets. 8th ICTP 347–348
11. Vanhove H, Gu J, Sol H, Duflou JR (2011) Process window extension for incremental forming through optimal work plane rotation. Special edition ICTP- Steel Res Int 508–512
12. Tanaka S, Hayakawa K, Nakamura T (2011) Incremental sheet forming with direction control of path planes. Special edition ICTP- Steel Research Int 503–507
13. Zhu H, Ju J, Bai JL (2018) Sheet thickness homogenization in CNC incremental forming based on tilted forming path. Comput Integr Manuf Syst 24(3):631–638
14. Vermaa A, Rajotiab S (2010) A review of machining feature recognition methodologies. Int J Comput Integr Manuf 23(4):353–368
15. Geng WZ, Chen ZM, He KJ, Wu YY (2016) Recognition for freeform machining feature of cavity parts. Comput Integr Manuf Syst 22(3):738–747
16. Xu S, Anwer N, Mehdi-Souzani (2015) Machining feature recognition from in-process model of NC simulation. Comput-Aided Des Appl 12(4):383–392
17. Wang J, Wang Z, Zhu W, Ji YF (2010) Recognition of freeform surface machining features. J Comput Inf Sci Eng 10(4):041006(1-7)
18. Keong CW, Yusri Y (2017) A Novel approach for automatic machining feature recognition with edge blend feature. MATEC Web of Conferences 135 00033(1-6)
19. Lingam R, Prakash O, Belk JH, Reddy NV (2016) Automatic feature recognition and tool path strategies for enhancing accuracy in double sided incremental forming. Int J Adv Manuf Technol 88(5):1639–1655
20. Zhu H, Li HY (2018) 5-Axis CNC incremental forming toolpath generation based on formability. Int J Adv Manuf Technol 94(1-4):1061–1072